

**Department of Mathematics**

# Well-posedness, Stability and Conservation for a Discontinuous Interface Problem

Cristina La Cognata and Jan Nordström

LiTH-MAT-R--2014/16--SE



**Linköpings universitet**  
**TEKNISKA HÖGSKOLAN**

Department of Mathematics  
Linköping University  
S-581 83 Linköping, Sweden.

# Well-posedness, stability and conservation for a discontinuous interface problem

Cristina La Cognata<sup>a</sup>, Jan Nordström<sup>b</sup>

<sup>a</sup>*Department of Mathematics, Computational Mathematics, Linköping University,  
SE-581 83 Linköping, Sweden ([cristina.la.cognata@liu.se](mailto:cristina.la.cognata@liu.se)).*

<sup>b</sup>*Department of Mathematics, Computational Mathematics, Linköping University,  
SE-581 83 Linköping, Sweden ([jan.nordstrom@liu.se](mailto:jan.nordstrom@liu.se)).*

---

## Abstract

The advection equation is studied in a completely general two domain setting with different wave-speeds and a time-independent jump-condition at the interface separating the domains. Well-posedness and conservation criteria are derived for the initial-boundary-value problem. The equations are semi-discretized using a finite difference method on summation-by-parts (SBP) form. The stability and conservation properties of the approximation are studied when the boundary and interface conditions are weakly imposed by the simultaneous approximation term (SAT) procedure. Numerical simulations corroborate the theoretical findings.

---

## 1. Introduction

In this paper we study fundamental properties such as well-posedness, stability and conservation for an advection equation, which changes wave-speed at an interface separating two spatial domains. The solution satisfies a time-independent jump-condition, which makes it discontinuous. Stability and conservation at interfaces have also been studied in [5],[6],[7] for the case of identical velocities in the two domains. We will extend that analysis by studying the problem in a completely general setting, where we vary the parameters related to the wave-speed and the jump condition in a controlled manner. Applications where this is of interest include acoustic electromagnetism, seismology and fluid dynamics, [23],[24],[25],[26],[27].

As our numerical approximation we will use high-order finite difference methods based on the SBP-SAT form [3],[4],[8],[21].

September 25, 2014

The rest of the paper proceeds as follows. In section 2 we study well-posedness and conservation properties of the continuous problem. Section 3 deals with the semi-discrete case. In section 4 we discuss the relation between the stability and conservation conditions of the schemes. A spectral analysis is performed in section 5, numerical calculations and verifications are presented in section 6. Finally, in section 7, we summarize and draw conclusions.

## 2. The discontinuous interface problem

Consider the Cauchy problem for the advection equation with two different real positive constant advection velocities

$$\begin{aligned} u_t + au_x &= 0, & x \leq 0, t \geq 0, \\ u_t + bu_x &= 0, & x > 0, t \geq 0, \\ u(x, 0) &= f(x), & x \in \mathbb{R}, t = 0. \end{aligned} \tag{1}$$

Without loss of generality we assume that both  $a, b$  are positive (opposite signs for the velocities make the domains uncoupled). Continuous solutions of (1) at the interface point  $x = 0$ , require

$$\lim_{x \rightarrow 0^+} u(x, t) = u^+(0, t) = u^-(0, t) = \lim_{x \rightarrow 0^-} u(x, t), \quad t \geq 0.$$

However this is a specific choice among many possible coupling conditions. We will consider the more general case

$$u^+(0, t) = cu^-(0, t), \quad t \geq 0$$

where  $c$  is a real constant which makes the solution discontinuous at the interface when it is different from one.

### 2.1. Well-posedness

We divide problem (1) into the following two coupled problems

$$\begin{aligned} u_t + au_x &= 0, & x \leq 0, t \geq 0, \\ u(x, 0) &= f_l(x), & x \leq 0, \end{aligned} \tag{2}$$

$$\begin{aligned} v_t + bv_x &= 0, & x \geq 0, t \geq 0, \\ v(x, 0) &= f_r(x), & x \geq 0, \\ v(0, t) &= cu(0, t), & t \geq 0. \end{aligned} \tag{3}$$

Our first result is

**Proposition 1.** *The coupled problem (2)-(3) are well-posed for any real constant  $c$ .*

*Proof.* The problem (2)-(3) is well-posed if a solution exists, is unique and has a bounded temporal growth, see [1],[19],[20] for more details about well-posedness. We apply the energy method by multiplying both sides of equations (2) and (3) with  $u$  and  $v$ , respectively. By considering only the boundary terms at the interface, integration by parts leads to

$$\frac{d}{dt} (\|u\|^2 + \alpha_c \|v\|^2) = u(0, t)^2 (-a + \alpha_c bc), \quad (4)$$

where  $\alpha_c$  is a positive free weight and  $\|\cdot\|$  indicate the standard  $L^2$ -norm. In order to get an energy estimate we require that

$$-a + \alpha_c bc \leq 0. \quad (5)$$

For  $c \leq 0$  any positive weight  $\alpha_c$  verifies (5). For  $c > 0$ , we find that  $\alpha_c \leq a/bc$ , satisfies (5). Time-integration of (4) with condition (5) leads to

$$\|u\|^2 + \alpha_c \|v\|^2 \leq \|f_l\|^2 + \alpha_c \|f_r\|^2. \quad (6)$$

Uniqueness of the solution can be proved by using the same technique. Suppose that two solutions of (2)-(3) exist with the same boundary and initial data, namely  $(u^{(1)}, v^{(1)})$  and  $(u^{(2)}, v^{(2)})$ . By linearity of the problem, the function  $(\bar{u}, \bar{v}) = (u^{(1)} - u^{(2)}, v^{(1)} - v^{(2)})$  is also a solution of (2)-(3) with homogeneous boundary, interface and initial conditions. By using the energy-estimate (6) with zero data we find  $(\bar{u}, \bar{v}) \equiv (0, 0)$ , i.e. the solution of (2)-(3) is unique.

Existence can be proved by using the Laplace transform technique for the initial boundary value problem, see [11],[12],[13] for details.  $\square$

## 2.2. Conservation

Consider the coupled problem (2)-(3) with the solution

$$w(x, t) = \begin{cases} u(x, t), & x \leq 0, t \geq 0 \\ v(x, t), & x \geq 0, t \geq 0 \end{cases} \quad (7)$$

of the slightly reformulated equation

$$w_t + \bar{u} w_x = 0 \quad t > 0 \quad (8)$$

where

$$\bar{u} = \begin{cases} a & x \leq 0, \\ b & x > 0 \end{cases}.$$

We multiply (8) by an arbitrary test function  $\phi(x, t) \in C^\infty$  with compact support. By integration with respect to space and time and using the interface condition, we get the following weak form of the original differential equation:

$$\int_{-\infty}^{\infty} [\phi w]_0^t dx - \int_{-\infty}^{\infty} \int_0^t [\phi_t + \phi_x \bar{u}] w dx dt + \int_0^t \phi u [a - bc]_{x=0} dt = 0.$$

Thus, all the terms at the interface vanish, resulting in a conservative problem if  $c = a/b$ . We summarize the result in the following Proposition.

**Proposition 2.** *The interface problem (2)-(3) is conservative if*

$$c = \frac{a}{b}. \tag{9}$$

**Corollary 1.** *The conservation condition (9) leads to well-posedness of (2)-(3) .*

*Proof.* By using  $\alpha_c = 1$  and inserting (9) into (4) we get

$$\frac{d}{dt} (\|u\|^2 + \|v\|^2) \leq 0.$$

Similar considerations about uniqueness and existence as in Proposition 1 lead to well-posedness.  $\square$

**Remark 1.** *Note that the converse of Corollary 1 is not true: well-posedness does not guarantee conservation.*

### 3. The semi-discrete approximation

The spatial derivative is discretized by using the technique based on summation-by-parts (SBP) finite difference operators introduced in [8],[9]. In this paper we use the standard SBP operator, even though more general

formulations exist, see for instance [28] and references therein. To be consistent with the continuous case in the following analysis we will ignore the outer boundary terms. The first derivative in space is approximated using

$$u_x \approx D\mathbf{u} = P^{-1}Q\mathbf{u},$$

where  $\mathbf{u} = (\dots, u_i, \dots)$  is the discrete grid function approximating the solution.  $P$  is a symmetric positive definite matrix,  $Q$  is almost skew-symmetric and satisfies the SBP property  $Q + Q^T = \text{diag}[-1, 0, \dots, 0, 1]$ . From now on we indicate the difference operator with  $P_{l,r}^{-1}Q_{l,r}$ , which are related to the left and right spatial intervals, respectively. We also introduce the grid vectors  $\mathbf{x}_l = [\dots, x_i, \dots, x_N = 0]$  and  $\mathbf{x}_r = [y_0 = 0, \dots, y_i, \dots]$ , that coincide at the interface point,  $x_N = y_0 = 0$ .

With this notation we can write the approximation of the systems (2)-(3) together with the SAT procedure [4],[5], for boundary and interface conditions as

$$\begin{aligned} \mathbf{u}_t + aP_l^{-1}Q_l\mathbf{u} &= P_l^{-1}\sigma_L(cu_N - v_0)e_N \\ \mathbf{v}_t + bP_r^{-1}Q_r\mathbf{v} &= P_r^{-1}\sigma_R(v_0 - cu_N)e_0, \end{aligned} \quad (10)$$

where, with a small abuse of notation, the vectors  $e_N = (0, \dots, 0, 1)$  and  $e_0 = (1, 0, \dots, 0)$  have the length of the left and right mesh, respectively. Note that  $v_0 \approx cu(0, t)$ .

### 3.1. Stability of the semi-discrete approximation

Similarly to the continuous case, we define two discrete  $L^2$  norms as follows

$$\|\mathbf{w}\|_{P_l} = w^T P_l w \quad \|\mathbf{w}\|_{P_r} = w^T P_r w. \quad (11)$$

We multiply both sides of (10) with  $\mathbf{u}^T P_l$ ,  $\mathbf{v}^T P_r$ , respectively, and add the corresponding transposes. By using the SBP properties of the discrete operators, we obtain

$$\frac{d}{dt} [\|\mathbf{u}\|_{P_l}^2 + \alpha_d \|\mathbf{v}\|_{P_r}^2] = \text{IT} \quad (12)$$

where  $\alpha_d$  is a positive weight (not necessarily the same as in the continuous case) and

$$\text{IT} = u_N^2(-a + 2c\sigma_L) + v_0^2\alpha_d(b + 2\sigma_R) - 2\sigma_L u_N v_0 - 2\alpha_d \sigma_R c u_0 v_N.$$

Next, we rewrite IT as a quadratic form given by

$$\text{IT} = \begin{pmatrix} u_N \\ v_0 \end{pmatrix}^T H \begin{pmatrix} u_N \\ v_0 \end{pmatrix}, \quad H = \begin{bmatrix} (-a + 2c\sigma_L) & -(\sigma_L + \alpha_d c \sigma_R) \\ -(\sigma_L + \alpha_d c \sigma_R) & \alpha_d(b + 2\sigma_R) \end{bmatrix}. \quad (13)$$

We have  $\text{IT} \leq 0$  if  $H$  is a negative semi-definite matrix. Hence, we need a condition on  $\sigma_L$  and  $\sigma_R$  to ensure that. The characteristic equation related to (13) is

$$\det(H - \lambda I) = \lambda^2 - \lambda(h_{11} + h_{22}) + (h_{11}h_{22} - h_{12}^2) = 0,$$

where  $h_{i,j}$   $i, j = 1, 2$  are the elements of  $H$ . By the properties of solutions to second order equations, we know that

$$h_{11} + h_{22} = \lambda_1 + \lambda_2 \quad (h_{11}h_{22} - h_{12}^2) = \lambda_1\lambda_2$$

Then  $\lambda_{1,2} \leq 0$  if  $h_{11} + h_{22} \leq 0$  and  $(h_{11}h_{22} - h_{12}^2) \geq 0$ . We can summarize the result as

**Proposition 3.** *The semi-discrete scheme (10) for the coupled advection equations (2)-(3) has a stable interface treatment when*

$$\begin{aligned} (-a + 2c\sigma_L) + \alpha_d(b + 2\sigma_R) &\leq 0, \\ (-a + 2c\sigma_L)\alpha_d(b + 2\sigma_R) - (\sigma_L + \alpha_dc\sigma_R)^2 &\geq 0. \end{aligned} \tag{14}$$

### 3.2. Conservation properties of the semi-discrete approximation

We define the vector function

$$\phi = (\phi_l, \phi_r) = (\dots, \phi_l(x_i), \dots, \phi_l(x_N), \phi_r(y_0), \dots, \phi_r(y_i), \dots), \tag{15}$$

with compact support and such that  $\phi_l(x_N) = \phi_r(y_0) = \phi(x_N)$ . Multiplying the equations in (10) by the discrete vectors  $\phi_l^T P_l$  and  $\phi_r^T P_r$ , respectively, we obtain

$$\begin{aligned} \phi_l^T P_l \mathbf{u}_t + a\phi_l^T Q_l \mathbf{u} &= \phi(x_N)\sigma_L(cu_N - v_0) \\ \phi_r^T P_r \mathbf{v}_t + b\phi_r^T Q_r \mathbf{v} &= \phi(x_N)\sigma_R(v_0 - cu_N). \end{aligned} \tag{16}$$

From the properties of  $Q_{l,r}$  it follows that for any vectors  $\mathbf{w}_l = (w_0, \dots, w_N)$ ,  $\mathbf{w}_r = (w_0, \dots, w_M)$  and  $\phi$  with compact support we have

$$\begin{aligned} \phi_l^T (Q_l + Q_l^T) \mathbf{w}_l &= \phi(x_N)(w_N)_l \\ \phi_r^T (Q_r + Q_r^T) \mathbf{w}_r &= -\phi(x_N)(w_0)_r. \end{aligned}$$

and hence (16) can be rewritten as

$$\begin{aligned} \phi_l^T P_l \mathbf{u}_t - a\mathbf{u}^T Q_l \phi_l &= -a\phi(x_N)u_N + \phi(x_N)\sigma_L(cu_N - v_0) \\ \phi_r^T P_r \mathbf{v}_t - b\mathbf{v}^T Q_r \phi_r &= +b\phi(x_N)v_0 + \phi(x_N)\sigma_R(v_0 - cu_N). \end{aligned} \tag{17}$$



We integrate (17) with respect to time and add the equations to obtain

$$\begin{aligned} & \phi_l^T P_l \mathbf{u}|_0^t + \phi_r^T P_r \mathbf{v}|_0^t = \\ & \int_0^t [\mathbf{u}^T P_l \phi_{l,t} + \mathbf{v}^T P_r \phi_{r,t} + a \mathbf{u}^T P_l (P_l^{-1} Q_l \phi_l) + b \mathbf{v}^T P_r (P_r^{-1} Q_r \phi_r)] dt + \\ & \int_0^t \phi(x_N) [u_N(-a + c\sigma_L - c\sigma_R) + v_0(b + \sigma_R - \sigma_L)] dt. \end{aligned}$$

We have a conservative scheme if the interface terms at  $x_N$  vanish, which require

$$-a + c\sigma_L - c\sigma_R = 0, \quad b + \sigma_R - \sigma_L = 0. \quad (18)$$

We have proved

**Proposition 4.** *The semi-discretization (10) with the continuous conservation condition (9) is a conservative approximation if*

$$\sigma_R = \sigma_L - b. \quad (19)$$

**Remark 2.** *Semi-discrete conservation for our problem requires a conservative continuous problem, since otherwise the system (18) has no solution. This is natural since any other result would have meant that an order one error had been committed.*

#### 4. The relation between stability and conservation

In section 2 we have shown well-posedness and derived the conservation condition for the interface problem (2)-(3) in the continuous case. In section 3 we derived stability and conservation conditions for the semi-discrete approximation of the same problem. All conditions are summarized below:

**The continuous case:**

- well-posedness  $\forall c \in \mathbb{R}$  (A1),
- conservation  $c = a/b$  (A2),

**The semi-discrete case:**

- stability

$$(-a + 2c\sigma_L) + \alpha_d(b + 2\sigma_R) \leq 0 \quad (\text{B1.a}),$$

$$(-a + 2c\sigma_L)\alpha_d(b + 2\sigma_R) - (\sigma_L + \alpha_dc\sigma_R)^2 \geq 0 \quad (\text{B1.b}),$$

- conservation

$$\sigma_R - \sigma_L + b = 0 \quad (\text{B2}).$$

Our problem is well-posed since (A1) always holds. We also demand stability by requiring that (B1.a,b) always holds.

#### 4.1. The non-conservative interface problem

We start by considering the most general well-posed interface problem and investigate stability without conservation. To have (B1.a) valid at the same time as (B1.b),  $(-a + 2c\sigma_L) \leq 0$  and  $(b + 2\sigma_R) \leq 0$  are required. This leads to

$$\sigma_L \leq \frac{a}{2c} \quad (\text{a}) \quad \text{and} \quad \sigma_R \leq \frac{-b}{2} \quad (\text{b}). \quad (20)$$

**Remark 3.** (B1.a) is also satisfied for  $|(-a + 2c\sigma_L)| \leq -|\alpha_d(b + 2\sigma_R)|$  but then (B1.b) cannot hold.

By adopting the variable  $\theta = 1/(\alpha_dc)$ , (B1.b) can be rewritten as the following second order inequality

$$-\theta^2\sigma_L^2 + 2\theta(b + \sigma_R)\sigma_L + \left[-\theta\frac{ab}{c} - 2\theta\frac{a}{c}\sigma_R - \sigma_R^2\right] \geq 0. \quad (21)$$

The inequality (21) can be associated to a second order equation for  $\sigma_L$  which is well-defined when the discriminant  $(b + 2\sigma_R)(b - \theta a/c)$  is non-negative. According to (20), this is true when  $(b - \theta a/c) \leq 0$ . Since the weight  $\alpha_d$  is a positive free parameter we can always make the choice  $\alpha_d \leq a/bc^2$  such that  $\theta \geq bc/a$  holds. Then, the inequality (21) is valid for

$$\frac{b + \sigma_R - \sqrt{(b + 2\sigma_R)(b - \theta(\frac{a}{c}))}}{\theta} \leq \sigma_L \leq \frac{b + \sigma_R + \sqrt{(b + 2\sigma_R)(b - \theta(\frac{a}{c}))}}{\theta}. \quad (22)$$

Next, we must compare (20.a) and (22) by letting  $\sigma_R = -b/2 - k/2$  with  $k \geq 0$ , we find

$$\frac{a}{2c} - \frac{b + \sigma_R + \sqrt{(b + 2\sigma_R)(b - \theta(\frac{a}{c}))}}{\theta} = \frac{\left(\theta\frac{a}{c} - b\right) + k - 2\sqrt{k\left(\theta\frac{a}{c} - b\right)}}{2\theta} \geq 0,$$

where we used that  $x + y \geq 2\sqrt{xy}$  for any  $x, y \geq 0$ .

We can conclude that conditions (20.b) and (22) are the relevant conditions and summarize the result in

**Proposition 5.** *The semi-discrete approximation (10) is stable for all parameters  $a, b, c$  when the penalty coefficients  $\sigma_L, \sigma_R$  satisfy (20.b) and (22).*

#### 4.2. The conservative continuous and non-conservative semi-discrete problem

Consider now the stability analysis for a conservative continuous interface problem by assuming that also condition (A2) is valid. Then, by letting  $c \rightarrow a/b$ , (20.b) remains unchanged while (22) becomes

$$\frac{b + \sigma_R - \sqrt{b(b + 2\sigma_R)(1 - \theta)}}{\theta} \leq \sigma_L \leq \frac{b + \sigma_R + \sqrt{b(b + 2\sigma_R)(1 - \theta)}}{\theta}. \quad (23)$$

In (23) we have used  $\theta = b/(a\alpha_d)$ . As in section 4.1, we can always choose  $\alpha_d \leq b/a$  such that  $\theta \geq 1$  holds. In particular if  $\alpha_d = b/a$  then  $\theta = 1$  and (23) becomes identical to (B2), i.e. the discrete conservation condition.

We have proved.

**Proposition 6.** *The continuous conservation condition (A2) leads to a stable semi-discrete approximation if the penalty parameters  $\sigma_L, \sigma_R$  satisfy (20.b) and (23).*

**Remark 4.** *Note that conservation and stability are two independent properties of the approximation (10). We have a stable and non-conservative semi-discretization if the assumptions of Proposition 6 are satisfied.*

**Remark 5.** *Note also that for one norm, the stability requirements in Proposition 6 also lead to conservation. That norm is given by  $\alpha_d = b/a$ .*

#### 4.3. The conservative continuous and semi-discrete problem

Consider the fully conservative case by assuming that (A2) and (B2) are both valid. Then (B1.a) leads to

$$\sigma_L \leq \frac{b}{2}. \quad (24)$$

By substituting (A2),(B2) and (24) into (B1.b) and following the same techniques as in the previous section, we obtain

$$\frac{b}{1 - \sqrt{\theta}} \leq \sigma_L \leq \frac{b}{1 + \sqrt{\theta}}, \quad (25)$$

where  $\theta = b/a\alpha_d$ . We can again choose  $\alpha_d \leq b/a$  such that  $\theta \geq 1$  holds. Note that as  $\theta \rightarrow 1^+$ , (25) converges from below to (24). Again (25) is more strict than (24). We have proved

**Proposition 7.** *The conditions (A2), (B2) and (25) leads to a stable and conservative scheme.*

**Remark 6.** *The choice  $\theta = 1$  makes (25) identical to (24).*

#### 4.4. The special case with continuous velocities

The result for a continuous advection velocity follows directly by going to the limit  $b \rightarrow a$  in (20.b) and (22). Thus, we get

$$\sigma_R \leq \frac{-a}{2}. \quad (26)$$

and

$$\frac{a + \sigma_R - \sqrt{a(a + 2\sigma_R)(1 - \frac{\theta}{c})}}{\theta} \leq \sigma_L \leq \frac{a + \sigma_R + \sqrt{a(a + 2\sigma_R)(1 - \frac{\theta}{c})}}{\theta}, \quad (27)$$

respectively, with  $\theta = 1/(\alpha_d c)$  and  $\alpha_d \leq 1/c^2$ . Furthermore, when  $c = 1$  then  $\alpha_d = \theta = 1$  and (27) converges to  $\sigma_L = \sigma_R + a$ , which is the conservation condition (B2) for a constant advection velocity derived in [4],[5],[6].

## 5. Spectrum analysis for stability at the interface

In this section we study the effect of the interface treatment on the continuous and semi-discrete spectrum.

### 5.1. Continuous and semi-discrete periodic boundary conditions.

Consider the discontinuous interface problem (2)-(3). To calculate the spectra of the problem we must restrict ourselves to a finite spatial domain, we choose  $[-1, 1]$ . To isolate the effect of the interface treatment, we introduce a periodic closure of the domains that removes the dissipative effect of the outer boundary terms. We use

$$u(-1, t) = dv(1, t) \quad t \geq 0. \quad (28)$$

By applying the energy method and using condition (28), we get

$$\frac{d}{dt} [\|\mathbf{u}\|^2 + \alpha_c \|\mathbf{v}\|^2] = \underbrace{v(1, t)^2(ad^2 - \alpha_c b)}_{(\text{BT})} + \underbrace{u(0, t)^2(-a + \alpha_c bc)}_{(\text{IT})}.$$

Then, for any  $\alpha_c$  which makes  $\text{IT} \leq 0$ , the choice  $d = \sqrt{\alpha_c b/a}$  removes the dissipative effect of the outer boundaries. In the rest of this section we always make this choice.

Consider the SBP-SAT approximation of (2)-(3), including condition (28)

$$\begin{aligned} \mathbf{u}_t + aP_l^{-1}Q_l\mathbf{u} &= P_l^{-1}[\sigma_{BL}(u_0 - dv_N)e_0 + \sigma_L(cu_N - v_0)e_N] \\ \mathbf{v}_t + bP_r^{-1}Q_r\mathbf{v} &= P_r^{-1}[\sigma_{BR}(dv_N - u_0)e_N + \sigma_R(v_0 - cu_N)e_0]. \end{aligned} \quad (29)$$

Now the discrete energy method leads to

$$\frac{d}{dt} [\|\mathbf{u}\|_{P_l}^2 + \alpha_d \|\mathbf{v}\|_{P_r}^2] = \text{IT} + \text{BT},$$

where IT is equal to the previously analyzed (13) and

$$\text{BT} = u_0^2(a + 2\sigma_{BL}) - 2u_0v_N(d\sigma_{BL} + \alpha_d\sigma_{BR}) + v_N^2\alpha_d(-b + 2d\sigma_{BR}).$$

By the choice

$$\sigma_{BL} = -\frac{a}{2}, \quad \sigma_{BR} = \frac{1}{2}\frac{b}{d} \quad \text{and} \quad d = \sqrt{\alpha_d \left(\frac{b}{a}\right)} \quad (30)$$

we obtain  $\text{BT}=0$  also for the semi-discrete energy estimate.

### 5.2. The continuous and semi-discrete spectrum.

To determine the continuous spectrum of (2)-(3), we use the Laplace transform technique [11],[12],[13]. The initial conditions are omitted since they do not contribute to the spectral analysis and we obtain

$$s\hat{u} + a\hat{u}_x = 0, \quad -1 \leq x \leq 0 \quad \text{and} \quad s\hat{v} + b\hat{v}_x = 0, \quad 0 < x \leq 1,$$

which have the general solutions

$$\hat{u} = c_l e^{-\frac{s}{a}x} \quad \text{and} \quad \hat{v} = c_r e^{-\frac{s}{b}x}.$$

The boundary and interface conditions lead to

$$E(s)\underline{c} = \begin{bmatrix} e^{\frac{s}{a}} & -de^{-\frac{s}{b}} \\ c & -1 \end{bmatrix} \begin{bmatrix} c_l \\ c_r \end{bmatrix} = 0. \quad (31)$$

The system of equations (31) has a non-trivial solution when the determinant of  $E(s)$  is zero, i.e. when  $\det(E(s)) = -e^{s/a} + cde^{-s/b} = 0$ . For  $cd \neq 0$  we get

$$s = \frac{ab}{a+b} [\log(|cd|) + 2i\pi k], \quad k \in \mathbf{Z}. \quad (32)$$

The infinite sequence (32) define the spectrum of (2)-(3) in combination with (28). Note that

- if  $|cd| = 1$  then we have purely imaginary spectrum,
- if  $|cd| > 1$  we have eigenvalues in the right half plane,
- if  $|cd| < 1$  we have eigenvalues in the left half plane.

To determine the corresponding semi-discrete spectrum we rewrite (29) in matrix form as

$$\begin{pmatrix} \mathbf{u} \\ \mathbf{v} \end{pmatrix}_t = P^{-1} \tilde{Q} \begin{pmatrix} \mathbf{u} \\ \mathbf{v} \end{pmatrix} \quad (33)$$

where

$$P = \begin{bmatrix} P_l & 0 \\ 0 & P_r \end{bmatrix}, \quad \tilde{Q} = -Q_\Lambda + \Sigma, \quad \text{and} \quad Q_\Lambda = \begin{bmatrix} aQ_l & 0 \\ 0 & bQ_r \end{bmatrix}.$$

The penalty matrix  $\Sigma$  which is zero everywhere except at the boundary and interface points is given by

$$\Sigma = \begin{bmatrix} \sigma_{BL} & & & & & -d\sigma_{BL} \\ & \ddots & & & & \\ & & c\sigma_L & -\sigma_L & & \\ & & -c\sigma_R & \sigma_R & & \\ & & & & \ddots & \\ -\sigma_{BR} & & & & & d\sigma_{BR} \end{bmatrix}.$$

The semi-discrete spectrum is given by the eigenvalues of  $P^{-1}\tilde{Q}$ .

By multiplying both sides of (33) with  $\bar{P} = \text{diag}(P_l, \alpha_d P_r)$  and adding the transpose we have

$$\frac{d}{dt} (\|\mathbf{u}\|_{P_l}^2 + \alpha_d \|\mathbf{v}\|_{P_r}^2) = \begin{pmatrix} \mathbf{u} \\ \mathbf{v} \end{pmatrix}^T [\tilde{\bar{Q}} + \tilde{\bar{Q}}^T] \begin{pmatrix} \mathbf{u} \\ \mathbf{v} \end{pmatrix},$$

where  $\tilde{\bar{Q}} = \bar{P}P^{-1}\tilde{Q}$ . By (30), the matrix  $\tilde{\bar{Q}} + \tilde{\bar{Q}}^T$  is non zero only at the interface block, which is the  $2 \times 2$  matrix given in (13). We can prove

**Proposition 8.** *The conditions (B1.a,b) implies that  $P^{-1}\tilde{Q}$  defined in (33) has eigenvalues with negative semi-definite real parts.*

*Proof.* Let  $\mathbf{x}$  be a complex eigenvector of the spatial operator  $P^{-1}\tilde{Q}$ . Then

$$\mathbf{x}^* \tilde{\bar{Q}} \mathbf{x} = \mathbf{x}^* \bar{P} P^{-1} \tilde{Q} \mathbf{x} = \mathbf{x}^* \bar{P} \lambda \mathbf{x} = \lambda \mathbf{x}^* \bar{P} \mathbf{x}, \quad (34)$$

where  $\lambda$  is the corresponding eigenvalue relative to  $\mathbf{x}$ . By applying the same procedure to  $\tilde{\bar{Q}}^T$  we get

$$\mathbf{x}^* \tilde{\bar{Q}}^T \mathbf{x} = \bar{\lambda} \mathbf{x}^* \bar{P} \mathbf{x}. \quad (35)$$

Summing (34) and (35) and recalling that  $\bar{P} > 0$  and diagonal, it follows that

$$\mathbf{x}^* [\tilde{\bar{Q}} + \tilde{\bar{Q}}^T] \mathbf{x} = (\lambda + \bar{\lambda}) \mathbf{x}^* \bar{P} \mathbf{x} = 2\text{Re}(\lambda) \mathbf{x}^* \bar{P} \mathbf{x}. \quad (36)$$

Hence,  $\text{Re}(\lambda) \leq 0$  since  $\tilde{\bar{Q}} + \tilde{\bar{Q}}^T \leq 0$ .  $\square$

## 6. Numerical results

Figure 1 show a few of the frames of the time-evolution between the initial time  $T = 0$  and  $T = 1.5$  of a conservative solution of (2)-(3). The initial data is zero in both domains. The boundary data is given by the function  $\sin(4\pi(-1 + 3t))$  and the wave is propagating with velocity  $a=2$  in the left domain and  $b=1$  in right domain. The jump condition satisfying (9) is  $c=2$ . The computations are done by using RK4 in time and SBP84, with CFL=0.1 and 300 grid points in each domain. The penalty  $\sigma_{L,R}$  satisfy the conservative assumptions of Proposition 7.

### 6.1. Accuracy

Next, we will establish the order of accuracy of our scheme. Consider the semi-discrete approximation (29). We choose

$$\begin{aligned} u_l(x, t) &= \sin(2\pi(x - t)) & -1 \leq x \leq 0, t \geq 0 \\ u_r(x, t) &= \cos(3\pi(x - 3t)) & 0 \leq x \leq 1, t \geq 0 \end{aligned} \quad (37)$$

as manufactured solutions. They satisfy the forced equations

$$\begin{aligned} (u_l)_t + a(u_l)_x &= F_l, & -1 \leq x \leq 0, t \geq 0 \\ (u_r)_t + b(u_r)_x &= F_r, & 0 \leq x \leq 1, t \geq 0 \end{aligned} \quad (38)$$

The solutions (37) are connected by the jump condition

$$u(0, t) - cv(0, t) = \sin(-2\pi t) - c \cos(-9\pi t) \quad (39)$$

and the periodic boundary conditions

$$u(-1, t) - dv(1, t) = \sin(2\pi(-1 + t)) - d \cos(3\pi(1 + t)). \quad (40)$$

In Table 6.1 we present the accuracy of SBP21, SPB42, SBP63 and SBP84 operators for a non-conservative problem and approximation (stability conditions from Proposition 5).

The rate of convergence  $p$  is computed by first calculating the error in the  $L^2$  and  $L^\infty$  norm of two approximations performed with  $N$  and  $2N$  points, respectively. Next we assume that the error is proportional to the spatial step to the power of  $p$ , which leads to  $p = \log_2(\text{Error}[N]/\text{Error}[2N])$ . Table 6.1 shows that the solutions computed with the considered SBP operators converge with  $2^{nd}$ ,  $3^{th}$ ,  $4^{th}$  and  $5^{th}$  order, respectively. We obtain analogous results for a conservative problem with both conservative and non-conservative approximation.



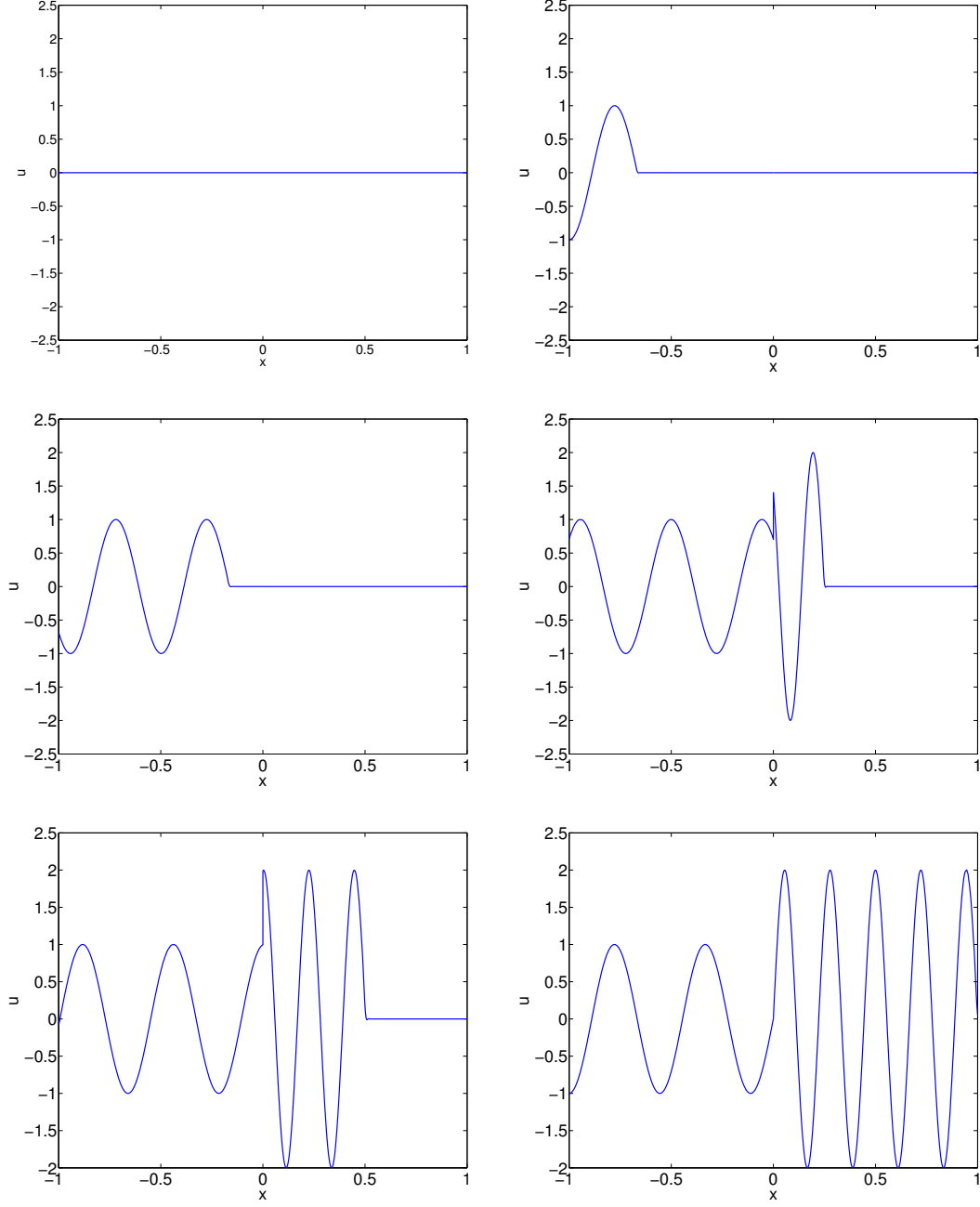


Figure 1: Time-evolution of a conservative solution of (2)-(3) between the initial time  $T = 0$  and  $T = 1.5$  with a conservative approximation (Proposition 7). The boundary condition is  $\sin(4\pi(-1+3t))$ . The parameters are:  $a=2$ ,  $b=1$  and  $c=2$ .

$L^2$	SBP21		SBP42		SBP63		SBP84	
N	$u_l$	$u_r$	$u_l$	$u_r$	$u_l$	$u_r$	$u_l$	$u_r$
40	1.9830	2.0915	3.2524	2.9650	5.2463	4.4964	5.8235	5.1834
80	2.0124	2.0267	3.0397	3.0096	3.6801	3.8770	4.5847	5.0897
160	2.0086	2.0102	3.0713	3.0083	3.8480	4.0149	4.7510	5.0624
320	2.0059	2.0044	3.0359	3.0068	3.9590	4.0052	4.9033	5.0176

$L^\infty$	SBP21		SBP42		SBP63		SBP84	
N	$u_l$	$u_r$	$u_l$	$u_r$	$u_l$	$u_r$	$u_l$	$u_r$
40	1.9201	1.9203	3.3609	3.1873	5.3065	4.0257	5.2865	5.3296
80	1.9856	2.0137	2.7951	3.0009	3.6586	3.7306	4.8152	4.8680
160	2.0349	2.0086	3.1082	3.0208	3.8312	4.2597	4.3987	5.0232
320	1.9931	2.0423	3.1472	3.0002	3.9057	4.1312	5.4902	4.9732

Table 1: Convergence rate as a function of grid N points for the non-conservative interface problem (38) and semi-discretization (29). Parameters setting: a=3, b=2, c=3. Interface penalties  $\sigma_{L,R}$  satisfying the stability conditions of Proposition 5.

## 6.2. The spectrum

Given that our numerical scheme is accurate, we now return to the analysis of the spectrum. We are interested in showing that the interface treatment produces a negative semi-definite spectrum for  $P^{-1}\tilde{Q}$ , which converges to the continuous spectrum. We are also interested in to what extent the conservation conditions derived earlier influence the spectrum.

Table 2 show the order of convergence for the semi-discrete spectra for SBP21, SPB42 and SBP63 operators. The convergence rate is computed by measuring the distance between the eigenvalues  $\lambda_i(N)$  from the semi-discrete spectrum of N of grid-points and the eigenvalues  $\lambda_i^c$  from the continuous spectrum. The index  $i$  refers to the magnitude of the imaginary part such that  $Imag(\lambda_i(N)) < Imag(\lambda_{i+1}(N))$ . We choose  $i$  small enough such that the numerical eigenvalue converge to the continuous one and we compute

$$Error(N) = |\lambda(N)_i - \lambda_i^c| \text{ for } i = 1, \dots, N, N = 40, 80, 160, \text{ and } 320.$$

The order of convergence is given by  $p = \log_2(Error(2N)/Error(N))$ . Note that Table 2 show that the convergence is the same as the order of the internal approximation.

N	SBP21	SBP42	SBP63	SBP84
40	2.4430	5.2086	6.1259	10.1153
80	2.0485	4.2217	6.9556	8.9885
160	2.0197	4.0813	5.9620	8.8797
320	2.0093	4.0369	6.0843	—

Table 2: Rate of convergence of semi-discrete eigenvalues of SBP21, SPB42, SBP63 and SBP84 operators. N indicates the number of grid points for each domain. The convergence is the same as the order of the internal approximation. The last  $N = 320$  result for SBP84 hit machine precision.

Figures 2.a-c show a number of comparisons between a semi-discrete and continuous spectrum. In Figures 2.a we have a non-conservative problem with  $a=2$ ,  $b=1$  and  $c=0.5$ . The penalty coefficients satisfy the stability conditions of Proposition 5. In Figure 2.b-c we have a conservative continuous problem with  $a=2$ ,  $b=1$  and  $c=a/b$ . In particular in Figures 2.b the penalty coefficients satisfy the non-conservative stability conditions of Proposition 6, i.e. the scheme is stable but non-conservative, while in Figures 2.c, they satisfy the conditions of Proposition 7, i.e. the scheme is stable and conservative. In all cases we use a  $4th$ -order accurate scheme. We can see that the spectra have eigenvalues with negative real parts, which implies well-posedness and a stable semi-discretization as stated in Proposition 8.

#### 6.2.1. Strict stability and artificial dissipation

All the plots in Figures 2.a-c show that all the eigenvalues of the discrete spectra are located in the left half plane, which was guaranteed by the energy stability formulated in Proposition 8. On the other hand, a few discrete eigenvalues are located to the right of the continuous spectrum. According to the definition of strictly stability, [1],[11],[12],[13], the time growth rate of a strictly stable approximation is bounded by the growth rate of the corresponding continuous problem. Hence, we prefer that the eigenvalues of the semi-discrete spectrum lies on the left side of the continuous spectrum. By adding suitable artificial dissipation terms to the semi-discretization (29), we can move the discrete spectrum to the left side of the continuous one without losing accuracy.

Figure 3 show the spectrum of the conservative approximation (29) using the SBP63 operator vs the continuous spectrum, with and without artificial

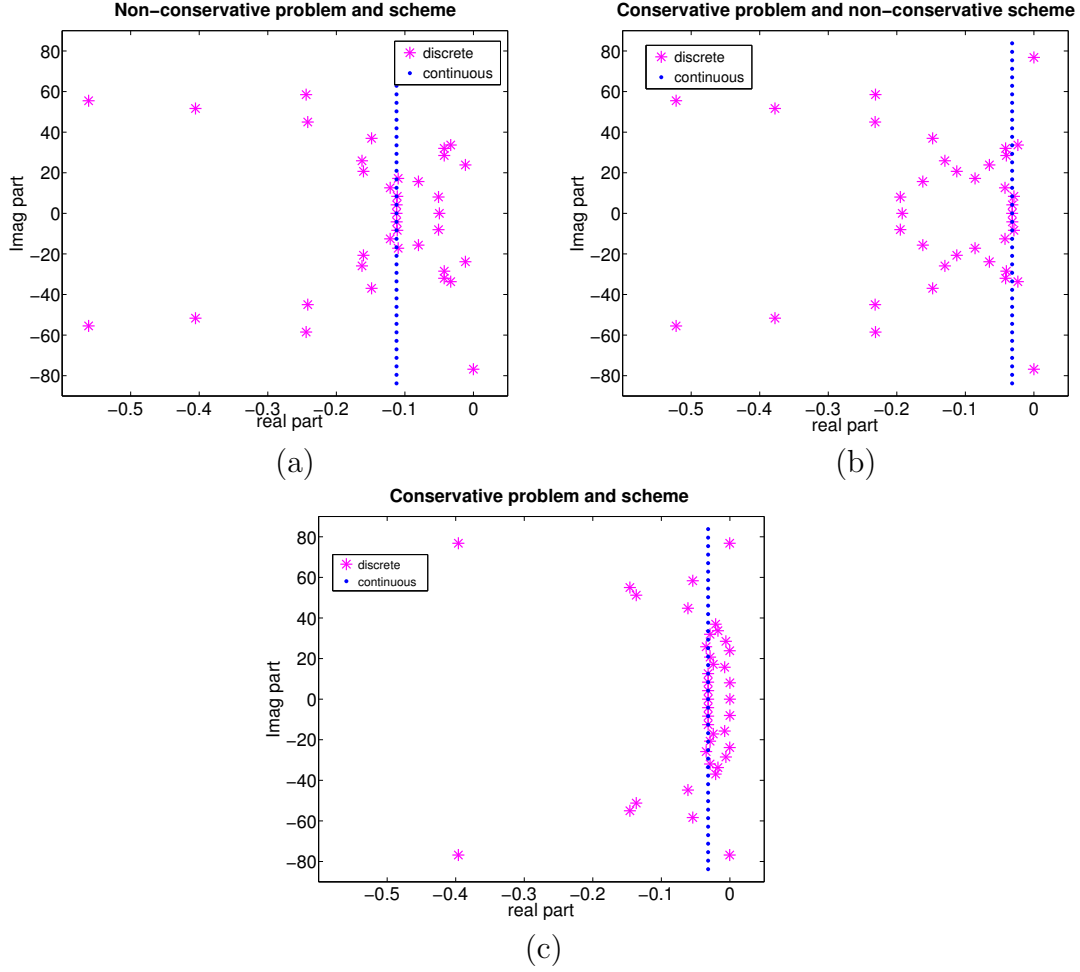


Figure 2: Continuous and semi-discrete spectrum of 4<sup>th</sup> order SBP-SAT approximation. Penalty coefficients  $\sigma_L, \sigma_R$  as in Proposition 5, (a), Proposition 6, (b), Proposition 7, (c).

N	SBP21	SBP42	SBP63	SBP84
40	2.0831	4.0950	6.1852	8.2203
80	2.0384	4.0542	6.1113	8.1961
160	2.0186	4.0288	6.0520	8.0825
320	2.0091	4.0148	6.0240	8.0325

Table 3: Rate of convergence of semi-discrete eigenvalues of SBP21, SPB42, SBP63 and SBP84 operators with artificial dissipation. N indicates the number of grid points for each domain. The order of convergence is not changed by introducing the artificial dissipation

dissipation. The semi-discrete eigenvalues in Figure 3.b converge from the left side implying strict stability. We get similar results for SBP21 and SBP42 operators and also for the non-conservative approximations. The rate of convergence is not changed by introducing the artificial dissipation, as can be seen in Table 3. For a discussion on how to build artificial dissipation operators for SBP operators without losing accuracy and stability, see [10]. The benefit of such operators on the spectrum has been also shown in [11].

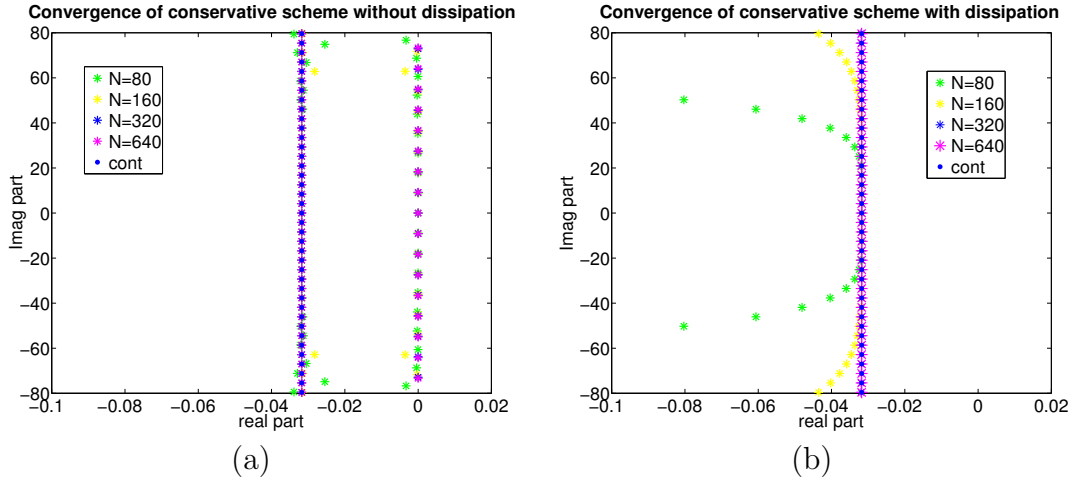


Figure 3: Close-up of the continuous and the semi-discrete spectrum of 4th order SBP-SAT approximation without dissipation, (a), and with dissipation, (b). Penalty coefficients  $\sigma_L, \sigma_R$  satisfy a conservative interface treatment as in Proposition 7. Parameter setting:  $a = 2$ ,  $b = 1$ , and  $c = 2$

### 6.2.2. The dissipative effect a conservative scheme for a conservative continuous problem

Figures 4.(a)-(f) show the spectra of conservative schemes vs spectra of a non-conservative type. In Figures 4.(a),(c) and (e) the scheme is stable and conservative, while in Figures 4.(b)-(d)-(f) the scheme is stable and non-conservative. In each row we have the same value of  $\theta$ , i.e. the same norm  $\alpha_d$ . In all cases we use a 4th-order accurate scheme. For  $\theta = 1$ , Figures 4(a-b), the spectra are identical since the stability conditions imply conservation, see (23) and (25). Note that in this case the scheme is automatically strictly stable since the discrete spectrum is completely located on the left side of the continuous one. In all the other examples we note that the non-conservative approximation has a few more eigenvalues on the right side of the continuous spectrum compared with the conservative approximation. This observation suggests that a non-conservative approximation is less dissipative than the conservative one.

We can check how dissipative the interface treatment is by considering the energy estimate (12). We recall that IT represents the effect of the interface treatment on the energy growth. We can measure how the interface treatment contributes to the estimate by computing the eigenvalues of the  $H$  in (13) which define the quadratic form IT.

In Figure 5 we show the eigenvalues  $h_1$  and  $h_2$  for different values of  $\theta$  for a non-conservative scheme (pink line) and a conservative scheme (green line). Note that the eigenvalues for the latter is always below the first one. This indicates that the conservative approximation is more dissipative than the non-conservative one.

## 7. Conclusions

We have presented a complete analysis of the discontinuous interface problem. We have shown that a such problem is always well-posed and we investigated when it is conservative.

We have derived a stable SBP-SAT scheme for a conservative and non-conservative continuous problem. In particular we have shown that for a conservative continuous problem we can choose between a conservative or non-conservative scheme with respect to a modified  $L^2$  norm.

We have also proved that a unique norm exists for which stability lead to conservation. Furthermore we have shown that the approximations can be made strictly stable by adding artificial dissipation without reducing the

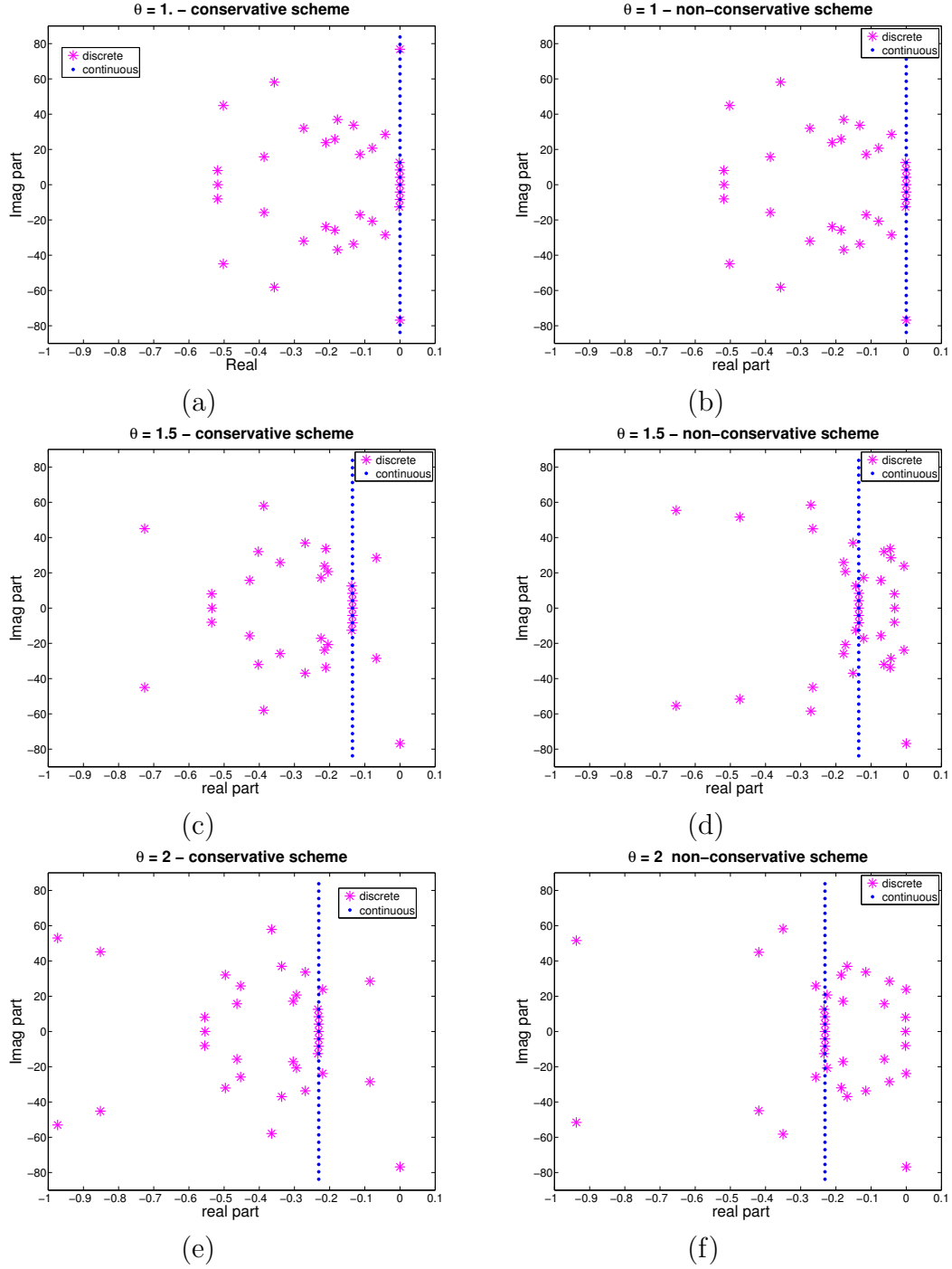


Figure 4: Comparison between conservative, (a),(c),(e), and non conservative, (b),(d),(f), semi-discrete spectra for a conservative continuous problem.

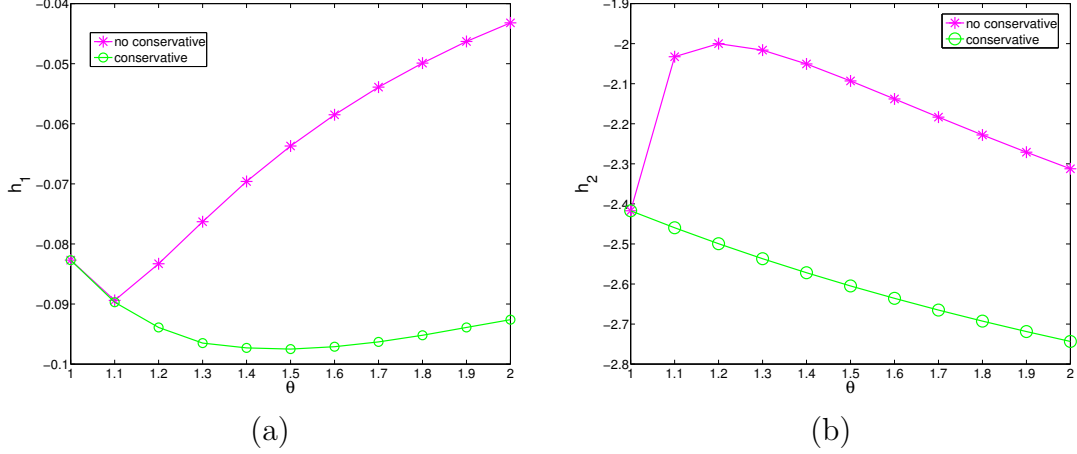


Figure 5: Trend of the eigenvalues  $h_1$ , (a), and  $h_2$ , (b), of  $H$  in (13) for different values of  $\theta$ . The pink pattern correspond to the non-conservative scheme, while the green one the conservative one. This latter is always below the first one which indicates that the conservative approximation is more dissipative than the non-conservative one.

accuracy. The schemes have been tested for accuracy and stability using numerical simulations with the method of manufactured solutions and a spectral analysis.

## References

- [1] Gustafsson, Kreiss, Oliger, *Time Dependent Problems and Difference Methods*, New York : Wiley & Sons (1995).
- [2] B. Gustafsson, *High Order Difference Methods for Time Dependent PDE*. Springer Series in Computational Mathematics (2008).
- [3] B. Strand, *Summation by parts for finite difference approximations for  $d/dx$* . Journal of Computational Physics, 110(1):47-67, 1994.
- [4] Mark H. Carpenter, David Gottlieb, and Saul Abarbanel. *Time-stable boundary conditions for finite-difference schemes solving hyperbolic systems: Methodology and applications to high-order compact schemes*. Journal of Computational Physics, 129, 1994.



- [5] Mark H. Carpenter, Jan Nordström, and David Gottlieb. *A stable and conservative interface treatment of arbitrary spatial accuracy*. Journal of Computational Physics, 148(2):341-365. (1999).
- [6] J. Gong and J. Nordström. *Interface procedures for finite difference approximations of the advection-diffusion equation*. Journal of Computational and Applied Mathematics, 236(5):602-620, 2011.
- [7] Mark H. Carpenter, Jan Nordström, and David Gottlieb. *Revisiting and Extending Interface Penalties for Multi-domain Summation-by-Parts Operators*. Journal of Scientific Computing 45:118-150, 2010.
- [8] Heinz-Otto Kreiss and Godola Scherer. *Finite element and finite difference methods for hyperbolic partial differential equations*. In Mathematical Aspects of Finite Elements in Partial Differential Equations, number 33 in Publ. Math. Res. Center Univ. Wisconsin, pages 195-212. Academic Press, 1974.
- [9] Heinz-Otto Kreiss and Godola Scherer. *On the existence of energy estimates for difference approximations for hyperbolic systems*. Technical report, Uppsala University, Division of Scientific Computing, 1977.
- [10] Ken Mattsson, Magnus Svård and Jan Nordström. *Stable and Accurate Artificial Dissipation*. Journal of Scientific Computing. Vol.21, No1, 2004
- [11] Jan Nordström. *Conservative Finite Difference Formulation, Variable Coefficients, Energy Estimates and Artificial Dissipation*. Journal of Scientific Computing. Vol.29, No. 3, 2006
- [12] B. Gustafsson, H.-O. Kreiss, A. Sundström. *Stability theory of difference approximations for mixed initial boundary value problems*. II, Mathematics of Computation 26 (119) 649-686, 1972
- [13] H.-O. Kreiss. *Stability theory of difference approximations for mixed initial boundary value problems*. I, Mathematics of Computation 22 (104) 703-714, 1968
- [14] Jan Nordström, *The influence of open boundary conditions on the convergence to the steady state for the Navier-Stokes equations*. Journal of Computational Physics, 85, pp:210-244 (1989).

- [15] Jan Nordström, Sofia Eriksson, Peter Eliasson, *Weak and strong wall boundary procedures and convergence to steady-state of the Navier-Stokes equations*, Journal of Computational Physics, 231, pp:4867-4884 (2012)
- [16] Jan Nordström, Sofia Eriksson, *Fluid Structure Interaction Problems: the Necessity of a Well Posed, Stable and Accurate Formulation*, Commun. Comput. Phys. Vol. 8, No. 5, pp:1111-1138 (2010).
- [17] P.J. Roache, *Code verification by the method of manufactured solutions*, Journal of Fluids Engineering, Transactions of the ASME 124, pp:4-10 (2002)
- [18] L. Shunn, F. Ham, P. Moin, *Verification of variable-density flow solvers using manufactured solutions*, Journal of Computational Physics 231 (2012) 3801-3827.
- [19] Jan Nordström, *The use of characteristic boundary conditions for the Navier-Stokes equation*, Computers and Fluids, Vol. 24, No. 5, pp:609-623. (1995)
- [20] Jan Nordström, Magnus Svärd, *Well-posed boundary conditions for the Navier-Stokes equation*, SIAM J. Numer. Anal. Vol. 43, No. 3, pp. 1231-1255. (2005)
- [21] Magnus Svärd, Jan Nordström *Review of summation-by-parts schemes for initial-boundary-value problems*, Journal of Computational Physics, 268, pp:17-38 (2014)
- [22] Roger A. Horn, Charles R. Johnson. *Matrix Analysis*. Second edition. Cambridge University Press (2013).
- [23] Ken Mattsson and Jan Nordström. *High order finite difference methods for wave propagation in discontinuous media*, Journal of Computational Physics, 200, pp. 249-269. (2006)
- [24] Jan Nordström and Rikard Gustafsson. *High Order Finite Difference Approximations of Electromagnetic Wave Propagation Close to Material Discontinuities*, Journal of Scientific Computing, Vol. 18, No. 2,(2003).

- [25] Jeremy E. Kozdon, Eric M. Dunham and Jan Nordström. *Simulation of Dynamic Earthquake Ruptures in Complex Geometries Using High-Order Finite Difference Methods*, Journal of Scientific Computing, Vol. 50, pp. 341-367 (2012).
- [26] Brittany A. Erickson and Jan Nordström. *Stable, high order accurate adaptive schemes for long time, highly intermittent geophysics problems*, Journal of Computational and Applied Mathematics, 271, pp. 328-338 (2014).
- [27] Jan Nordström, Jing Gong, Edwin van der Weide and Magnus Svärd. *A stable and conservative high order multi-block method for the compressible Navier-Stokes equations*, Journal of Computational Physics, 228, pp. 9020-9035 (2009).
- [28] David C. Del Rey Fernández, Pieter D. Boom and David W. Zingg. *A generalized framework for nodal first derivative summation-by-parts operators* Journal of Computational Physics archive, Vol 266, pp. 214-239 (2014).